THE EFFECT OF ADDITIVES ON THE SIZE OF Fe_3O_4 PARTICLES

W.L. Tan and M. Abu Bakar*

Nanoscience Research Laboratory, School of Chemical Sciences,
Universiti Sains Malaysia, 11800 USM Pulau Pinang, Malaysia

*Corresponding author: bmohamad@usm.my

Abstract: *The study on the effect of different additives on the size and size uniformity of magnetite (Fe_3O_4) nanoparticles is described. The magnetite particles are characterized by Fourier Transform Infrared (FTIR) and X-ray diffraction (XRD). The X-ray powder diffraction patterns and IR spectra of the as-formed magnetite particles indicate additive-free products were obtained. Analyses on the size and size distribution of the magnetite obtained suggest that the additives – surfactants, chitosan and inorganic ligands have different manipulating ability. Surfactants gave better manipulation on particle size (ca. < 45 nm) as well as the size distribution (ca. SD < 20 nm). Chitosan can manipulate the size distribution while maintaining the average size of the original magnetite. Whereas inorganic ligands, with the exception of thiourea, exert only slight influence on the size distribution with no manipulation over the average size. Transmission electron microscopy (TEM) micrographs suggest that citrate and stearic acid may have affected the final morphology of the magnetite formed in their presence.*

Keywords: magnetite, particles' size, surfactants, chitosan, nanoparticles

1. INTRODUCTION

Ferromagnetic oxides, mostly magnetite, Fe_3O_4 and maghemite, γ-Fe_2O_3 form an interesting class of nanomaterials. They have been extensively studied recently due to their unique physical, chemical, thermal and mechanical properties [1]. Iron oxides are used in broad range of applications including biomedical [1,2], adsorbent [3], catalysis [4,5], magnetic storage devices [6], magnetic refrigeration systems [7], and passivation coatings [8] among others.

Magnetite is a common magnetic iron ore, comprise of 72.36% iron and 27.64% oxygen exhibits high electronic conductivity due to its inverse spinel structure [9,10]. To date, magnetite is known to be low in toxicity and is biocompatible. These features make it an ideal element for in vitro diagnostics [1]. Nanosize magnetite behaves as superparamagnet and has been applied in magnetic resonance imaging (MRI) as contrast agent [11]. Lately, numerous attempts of synthesizing and characterizing magnetite nanoparticles have been

reported. Chemical co-precipitation [12], forced hydrolysis [13], DC plasma jet method [14], solvothermal [15] and sonochemical [11] reductions have been successfully employed.

The properties of nanomaterials are strongly dependent on their size, morphology and preparative method [16]. In order to exert these features, additives or stabilizers such as surfactants, polymers, ligands or dendrimers are usually included in the preparative procedure. In the present work, the effect on size and size distribution of magnetite nanoparticles by using different additives is evaluated. In addition, the morphological outcome of the as-formed particles is also discussed.

2. EXPERIMENTAL PROCEDURE

2.1 Materials and Equipments

The following commercially available materials were used without further purification – chitosan of medium molecular weight ~400000, stearic acid, acetic acid 99.8%, iron(II) sulphate, potassium hydroxide, potassium nitrate, sodium dodecylsulphate (SDS) 99%, Triton-X 100, N-Cetyl-N,N,N-trimethylammonium bromide (CTAB), tri-n-octylphosphinoxide (TOPO), trisodium citrate and thiourea.

The FTIR spectra were recorded using Thermo Nicolet IR200 spectrometer. The dried samples were ground with KBr and pressure pressed into a pellet. The spectra were collected in the region of 400 to 4000 cm^{-1}. The transmission electron microscopy (TEM) micrographs of the samples were obtained using Philip CM 12 TEM operating at 80 kV. One mg of sample was dispersed in 5 ml of 3:2 ethanol:deionized water mixture and sonicated for 15 minutes. A drop of dispersion was placed on a carbon coated copper grid and the solvent was evaporated off. The particles diameters were measured and analyzed using a computer program Analysis Docu version 2.11 (GMBH). The average particle size and size distribution were obtained from ≥ 500 particles. Standard deviation (σ) of the sample is calculated according to the formula:

$$\sigma^2 = \Sigma(x_i - x)^2 / N.$$

All samples were characterized by powder X-ray diffraction (XRD). Data were collected on a SIEMENS D5000 X-ray diffractometer with monochromatic Cu-Kα radiation filter in the 2θ range from 0–100º.

2.2 Preparation of Fe_3O_4 Nanoparticles

Magnetite particles were synthesized with modification of the method reported by Bruce et al. [17]. Solutions of iron(II) sulphate heptahydrate (1.67 g, 6×10^{-3} mol) in 50 ml deionized water, potassium nitrate (1.01 g, 1×10^{-2} mol) in 10 ml of deionized water, and 2.5 M potassium hydroxide were prepared. 1% (w/w) stabilizer was mixed with the iron salt solution under vigorous stirring for two hours. To this solution, potassium nitrate was added and stirring was continued for another half an hour. Then, 10 ml of 2.5 M potassium hydroxide (2.5×10^{-2} mol) was slowly added to the above solution. The reaction mixture was heated to 100°C under nitrogen and maintained at this temperature for two hours. The nitrogen flow was then turned off and the mixture was cooled down to room temperature. After cooling, the black precipitate was repeatedly washed with deionized water, centrifuged and allowed to dry under vacuum at 50°C overnight.

Similar experiments were repeated using various stabilizers including CTAB, SDS, Triton X100, stearic acid, TOPO, trisodium citrate, thiourea and chitosan. A similar experiment without any additive added was also carried out.

3. RESULTS AND DISCUSSION

3.1 Characterization

3.1.1 FTIR spectrum

All FTIR spectra of synthesized iron oxides with and without stabilizers as in Figure 1, show a broad band at ~570 cm^{-1} as tabulated in Table 1. The spectra were found consistent with that reported by Bruce et al. [17] of pure magnetite (Fe_3O_4). There is little or no indication of other iron oxide impurities as detected from the spectra of the products obtained.

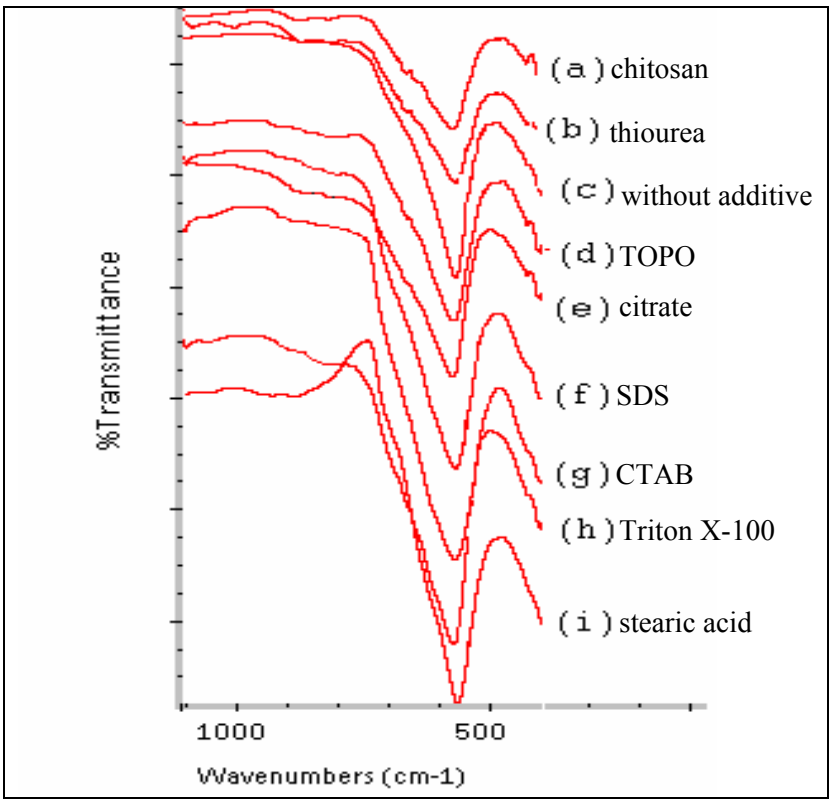

Figure 1: FTIR spectra (400–1100 cm^{-1}) of magnetite synthesized with and without additives

Table 1: Size and IR band of magnetite particles prepared in various additives

Types of additive	Additive	ν_s (Fe_3O_4)/cm^{-1} (Δ)*	Size and SD of particles/nm
Surfactant	Stearic acid	565.4 (–4.0)	33.9 ± 11.6
	CTAB	570.2 (+0.9)	35.3 ± 15.8
	Triton X-100	573.1 (+3.8)	39.6 ± 17.7
	SDS	569.6 (+0.3)	43.4 ± 15.8
Polymer	Chitosan	575.9 (+6.6)	65.4 ± 17.2
Ligand	thiourea	569.4 (+0.1)	60.2 ± 20.3
	TOPO	573.4 (+6.0)	91.4 ± 29.3
	Citrate	575.6 (+6.3)	118.8 ± 47.3
None added	Nil	569.3 (–)	57.2 ± 74.9

Note: * Δ = [ν_s (Fe_3O_4) without additive] – [ν_s (Fe_3O_4) with additive]

3.1.2 XRD

All powder diffractograms of the synthesized magnetites clearly show that all diffraction peaks of each sample matched the diffraction peaks for pure magnetite (Fe_3O_4) from the reference database (JCPDS File No. 19-629). The six most intense peaks corresponding to the Miller indices for the reflection planes (220), (311), (400), (422), (511) and (440) at 30.3º, 35.6º, 43.2º, 53.6º, 57.1º and 62.8º**,** respectively were clearly observed. Representative XRD patterns of these magnetites are shown in Figure 2. The XRD results also confirmed the purity of the products via the absence of other phases of iron oxide such as maghemite or hematite in samples.

3.2 TEM Analyses

3.2.1 Size and size distribution

The average size and standard deviation (SD) of the prepared magnetite particles are tabulated in Table 1. Figure 3 shows the size distribution of magnetite particles prepared in various additives. Generally, the additives have a significant influence on the size and size distribution of resultant products. In relation to the normally prepared magnetite, the type of additives used can be divided into three categories based upon the size and size distribution of the product magnetite they influenced. These are surfactants, chitosan and the inorganic ligands.

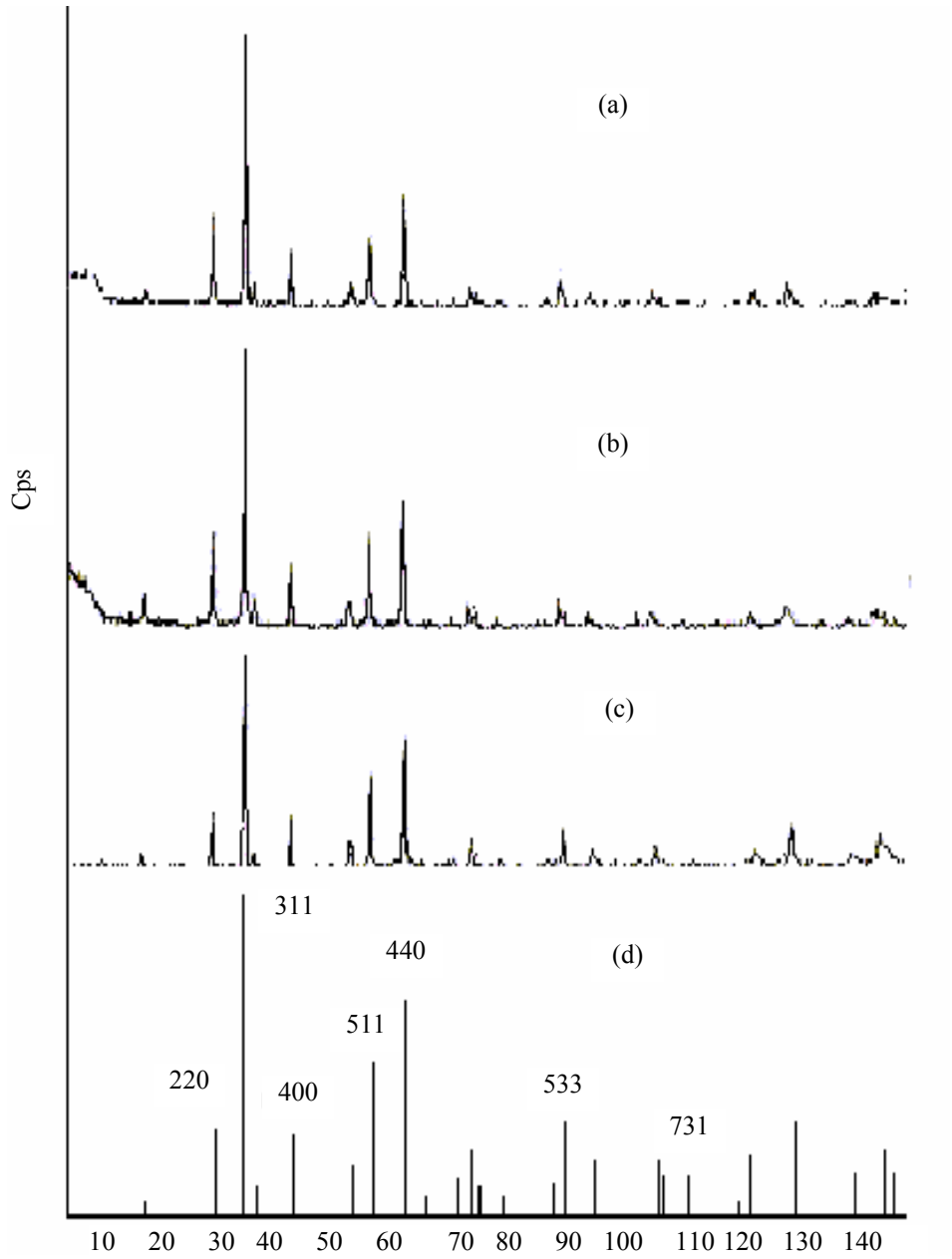

Figure 2: Representative XRD patterns of magnetite prepared (a) with SDS, (b) with citrate, (c) without additive, and (d) reference (JCPDS File No. 19-629)

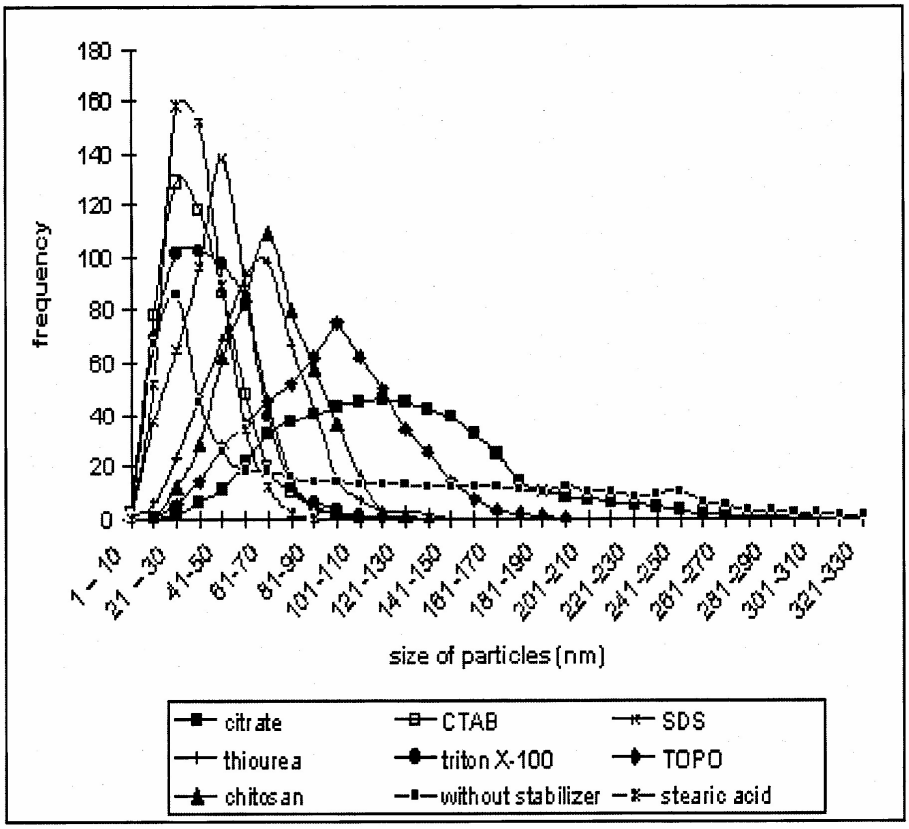

Figure 3: Size distribution of as-prepared magnetite particles in various additives

Without any additives, the as-synthesized magnetite particles were a mixture of small individual particles and aggregates distributed over a wide range of sizes as indicated by the large standard deviation (SD = 74.9 nm). It is well known that without any surface coating, magnetite particles tend to agglomerate to form large clusters due to the hydrophobic interactions between particles surfaces [1]. In contrast, when additives such as surfactants, ligands or chitosan were added during the preparation process, the size distribution of the as-formed particles can be controlled at SD below 50 nm. Thus additives play a crucial role in protecting the newly born particles from rapid flocculation, thus inhibiting the agglomeration of particles [18].

Long chain surfactants gave better manupulation on the particles' size as well as the distribution with an overall particles' size in the range of 20 to 60 nm.

Most surfactants are known to have long hydrocarbon chain structures with hydrophobic ends. It is believed that this structure is critical in manipulating magnetite particle sizes. These long chains act as a barrier, which protect the particles and cause a steric hindrance that restricts the growth of particles. Anionic surfactants such as stearic acid and SDS will form complex with Fe^{2+} during reaction via ionic bonds [19,20]. Strong ionic repulsion forces between complexes prevent close contact of magnetite particles thus affording controls on the particles' sizes [21]. Triton X-100, a non-ionic surfactant bearing polyoxyethylene (POE) chain, which can attract Fe^{2+} via dipole-ion interactions result in positively charged complexes [22]. These complexes will then restrict growth of the magnetite particles through charge repulsion as well as via protection through the formation of polymer helical structures on the particle surfaces. However, CTAB, a cationic surfactant would not form complex with Fe^{2+}. Nevertheless, it can adsorb on magnetite surface via the headgroup and form a bilayer structure, which acts as a barrier to prevent the agglomeration of particles [23].

Chitosan, a natural polymer contains hydroxyl and amino groups that may serve as cationic or anionic sites. Complexation between chitosan and the metal ions usually involves the amine group [24]. Nevertheless, the affinity of ferric or ferrous ions for amine is low [25]. Thus, we believe that the size manipulation on the as-formed particles was attributed to the constrained growth of particles in nano-voids. Many polymers contain nano-voids in their structure naturally. The number and sizes of such voids are specific to each polymer matrix. The particles grew simultaneously in the cavities with the consequent particle sizes governed by the sizes of these nano-voids [26].

Magnetite particles formed in the presence of TOPO or sodium citrate gave larger average sizes with a wider distribution as compared to the surfactants or chitosan. According to Hou et al. [27] TOPO cannot prevent nanoparticles aggregation if it is used alone. It may be due to the weak coordination between the phospine oxide moieties with metal oxide surfaces. Citrate has strong influence on the size and structure of particles depending on its concentration [28]. In our case, the molar ratio between iron salt to citrate is around 105 to 1. It is clearly noted that the quantity of citrate used in this work is too low to coordinate with Fe^{2+} efficiently. As for thiourea, it can restrict the size of magnetite particles to an average size of 60.2 nm by entrapping it through sulphur donors [29].

3.2.2 Morphology

Without additives, the synthesized magnetite particles were crystalline and they tended to be a mixture of a few identifiable shapes as well as some undistinguished geometries. Figure 4 depicts some of magnetite particles obtained without the use of additive. It clearly showed that they have distinctive outlines such as triangle, circle, rectangle and square. Particles are free to grow from any surfaces or planes without inhibition by the additive. This thus gives rise to different shaped particles.

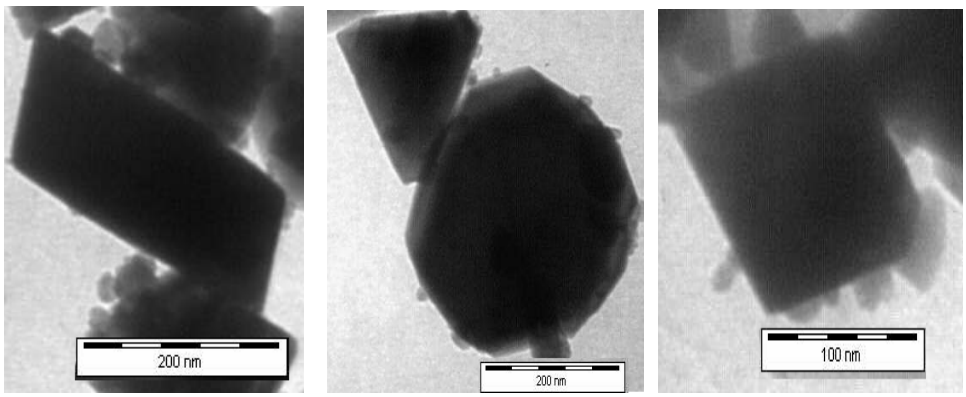

Figure 4: TEM micrographs of magnetite particles prepared without additive

Additives act as capping agents and can exert a strong influence on the shape of as-formed particles by governing the growth rate of various crystallographic surfaces and create orientations in crystals formation [30]. With the exception of trisodium citrate and stearic acid, this study has shown that most of the magnetite particles, as shown in Figures 5 (a)–(f) displayed shapes of the sharp edge quadrates when additives were used in the preparation. These quadrates could be decahedra, which is orientated with the five-fold axis parallel to the substrate plane (001) as reported previously [31].

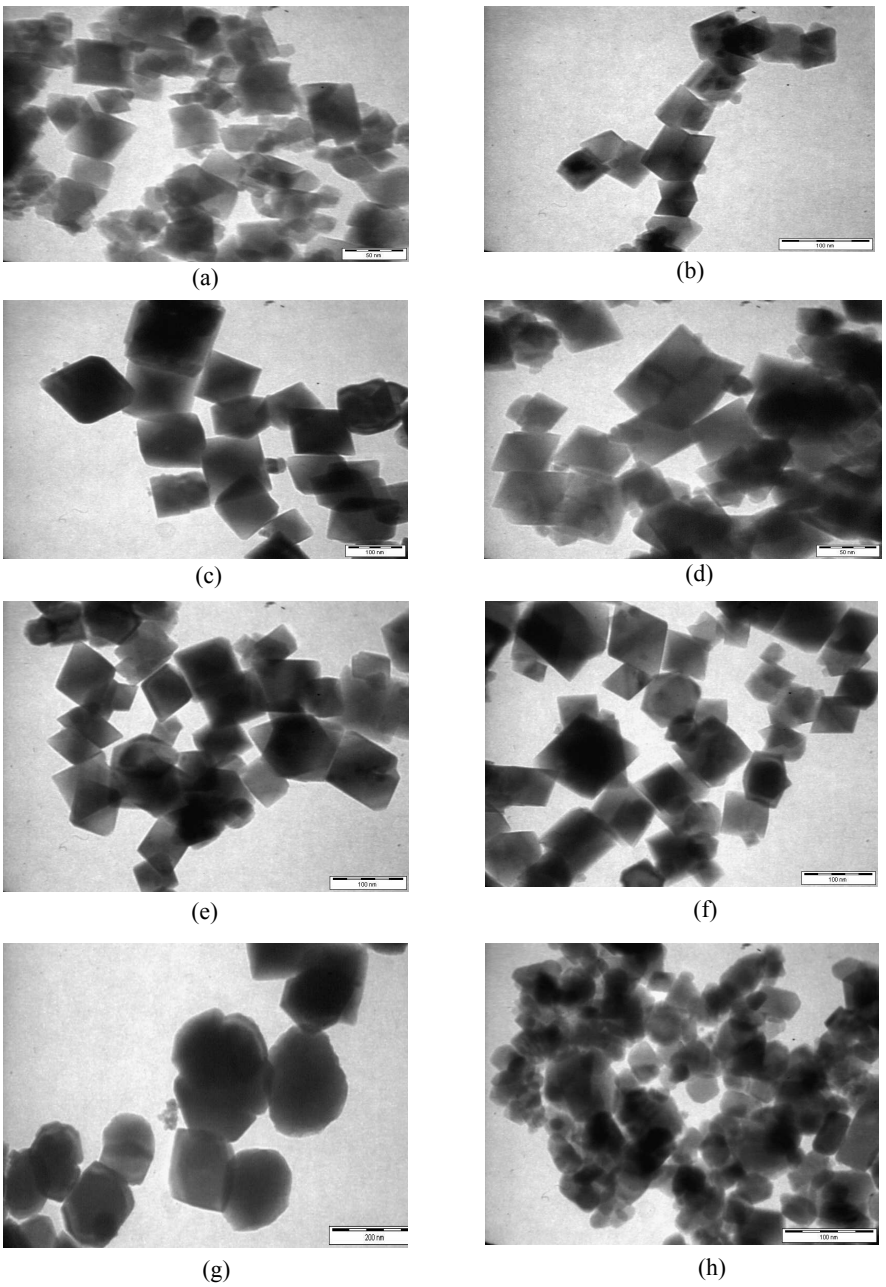

Figure 5: TEM micrographs of magnetite particles synthesized with (a) CTAB, (b) SDS, (c) TOPO, (d) triton X-100, (e) chitosan, (f) thiourea, (g) citrate, and (h) stearic acid

As shown in Figure 5(g), the magnetite particles appeared to be bigger and more rounded in shape with some defects when citrate is the additive. These defects have been explained by Henglein et al. [28]. The lack of protection on the particles surfaces induce tendency to coalesce and produce all the dislocations in the particles. Henglein et al. [28] have found that at low citrate concentrations, as-formed particles tended to coadunate and create imperfections such as the multiply twinned particles. However, when stearic acid was used, majority of magnetite particles show pseudo-trigonal and truncated octahedral as depicted in Figure 5(h). The particles became more rounded in shape when truncations are introduced to it. According to Yacaman et al. [32], the truncations occur in order to reduce the surface energy of the particles therefore making the resultant particles more stable.

4. CONCLUSIONS

The size, size distribution and to some extent the morphology of the as-formed magnetite nanoparticles are dependent on the nature of additives that may be surfactants, chitosan or inorganic ligands. Surfactants afford the smallest size as well as narrow size distribution of magnetite particles as indicated by their SD. The size distribution can be manipulated via the SD of up to five-fold decrease as compared to those without using any additive. Due to its long chain structure, it can prevent further particle growth by forming an effective barrier surrounding the particles. As for chitosan, the magnetite exhibits comparable size to that obtained without any additives but the size distribution is controllable similar to that of the surfactants. This can be attributed to the nano-voids created within the chitosan matrix. However, in the case of inorganic ligands, they can only manipulate the size distribution but not the average size of the particles as compared to magnetite prepared without any additives.

5. ACKNOWLEDGEMENT

This work was supported by USM grant FRGS (203/PKIMIA/670049).

6. REFERENCES

1. Gupta, A.K. & Gupta, M. (2005). Synthesis and surface engineering of iron oxide nanoparticles for biomedical applications. *Biomaterials*, 26, 3995–4021.
2. Fink, A.P., Chastellain, M., Jeanneret, L.J., Ferrari, A. & Hofmann, H. (2005). Development of functionalized superparamagnetic iron oxide

nanoparticles for interaction with human cancer cells. *Biomaterials*, 26, 2685–2694.

3. Liao, M.H. & Chen, D.H. (2002). Fast and efficient adsorption/ desorption of protein by a novel magnetic nano-adsorbent. *Biotechnology Lett.*, 24, 1913–1917.
4. Takenaka, S., Kaburagi, T., Yamada, C., Nomura, K. & Otsuka, K. (2004). Storage and supply of hydrogen by means of the redox of the iron oxides modified with Mo and Rh species. *J. Catalysis*, 228, 66–74.
5. Pestman, R., Koster, R.M., Boellaard, E., van der Kraan, A.M. & Ponec, V. (1998). Identification of the active sites in the selective hydrogenation of acetic acid to acetaldehyde on iron oxide catalysts. *J. Catalysis*, 174, 142–152.
6. Kim, D.K., Mikhaylova, M., Zhang, Y. & Muhammed, M. (2003). Protective coating of superparamagnetic iron oxide nanoparticles. *Chem. Mater.*, 15, 1617–1627.
7. Hyeon, T. (2003). Chemical synthesis of magnetic nanoparticles. *Chem. Comm.*, 927–934.
8. Yi, W., Moberly Chan, W., Narayanamurti, V., Hu, Y.F., Li, Q., Kaya, I. Burns, M. & Chen, D.M. (2004). Characterization of spinel iron-oxide nanocrystals grown on Fe wiskers. *J. Appl. Phys.*, 95, 7136–7138.
9. Poveromo, J.J. (1999). *Ironmaking volume*. Pittsburgh: The AISE Steel Foundation, 547–550.
10. Wells, A.F. (1975). *Structural inorganic chemistry* (4th ed.). UK: Oxford University Press, 456.
11. Kim, E.H., Lee, H.S., Kwak, B.K. & Kim, B.K. (2005). Synthesis of ferrofluid with magnetic nanoparticles by sonochemical method for MRI contrast agent. *J. Magn. Mater.*, 289, 328–330.
12. Zhang, H., Wang, R., Zhang, G. & Yang, B. (2003). A covalently attached film based on poly(methacrylic acid)-capped Fe_3O_4 nano-particles. *Thin Solid Films*, 429, 167–173.
13. Huang, Z., Tang, F. & Zhang, L. (2005). Morphology control and texture of Fe_3O_4 nanoparticle-coated polystyrene microspheres by ethylene glycol in forced hydrolysis reaction. *Thin Solid Films*, 471, 105–112.
14. Todaka, Y., Tsuchiya, K., Umemoto, M., Sasaki, M. & Imai, D. (2003). Growth of Fe_3O_4 whiskers from solid solution nanoparticles of Fe-Cu and Fe-Ag systems produced by DC plasma jet method. *Mater. Sci. Eng. A*, 340, 114–122.
15. Hou, Y., Yu, J. & Gao, S. (2003). Solvothermal reduction synthesis and characterization of superparamagnetic magnetite nanoparticles. *J. Mater. Chem.*, 13, 1983–1987.
16. Wang, D., Song, C., Gu, G. & Hu, Z. (2005). Preparation of Fe_2O_3 microcages from the core/shell structures. *Materials Letters*, 59, 782–785.

17. Bruce, I.J., Taylor, J., Todd, M., Davies, M.J., Borioni, E., Sangregorio, C. & Sen, T. (2004). Synthesis, characterization and application of silica-magnetite nanocomposites. *J. Magn. Magn. Mater.*, 284, 145–160.
18. Lee, J., Isobe, T. & Senna, M. (1996). Preparation of ultrafine Fe_3O_4 particles by precipitation in the presence of PVA at high pH. *J. Colloid & Interface Sci.*, 177, 490–494.
19. Wohrle, D. & Pomogailo, A.D. (2003). *Metals complexes and metals in macromoloecules – Synthesis*, *structure and properties*. Weinheim, Germany: Wiley-VCH, 195.
20. Wu, X., Wang, D. & Yang, S. (2000). Preparation and characterization of stearate-capped titanium dioxide nanoparticles. *J. Colloid & Interface Sci.*, 222, 37–40.
21. Abu Mukh-Qasem, R. & Gedanken, A. (2005). Sonochemical synthesis of stable hydrosol of Fe_3O_4 nanoparticles. *J. Colloid & Interface Sci*., 284, 489–494.
22. Hagerstrand, H., Bobacka, J., Hagerstrand, M.B., Iglic, V.K., Fosnaric, M. & Iglic, A. (2001). Oxyethylene chain-cation complexation; nonionic polyoxyethylene detergents attain a positive charge and demonstrate electrostatic head group interactions. *Cellular & Molecular Bio. Lett.*, 6, 161–165.
23. Wu, S.H. & Chen, D.H. (2004). Synthesis of high-concentration Cu nanoparticles in aqueous CTAB solutions. *J. Colloid & Interface Sci.*, 273, 165–169.
24. Park, J.W., Park, M.O. & Park, K.K. (1984). Mechanism of metal ion binding to chitosan in solution. Cooperative inter- and intramolecular chelations. *Bull. Korean Chem. Soc.*, 5, 108–112.
25. Albert Cotton, F., Wilkinson, G. & Gaus, P.L. (1987). *Basic inorganic chemistry* (2nd ed.). New York: Wiley, 496.
26. Gubin, S.P. (2002). Metal containing nano-particles within polymeric matrices: Preparation, structure, and properties. *Coll. & Surf. A: Phyiscochem. Eng. Aspects*, 202, 155–163.
27. Hou, Y., Kondoh, H., Ohta, T. & Gao, S. (2005). Size-controlled synthesis of nickel nanoparticles. *Applied Surface Sci.*, 241, 218–222.
28. Henglein, A. & Giersig, M. (1999). Formation of colloidal silver nanoparticles: Capping action of citrate. *J. Phys. Chem. B*, 103, 9533–9539.
29. Dixit, S.G., Mahadeshwar, A.R. & Haram, S.K. (1998). Some aspects of the role of surfactants in the formation of nanoparticles. *Coll. & Surf. A: Physicochem. Eng. Aspects*, 133, 69–75.
30. Qian, C., Kim, F., Ma, L., Tsui, F., Yang, P. & Liu, J. (2004). Solution-phase synthesis of single-crystalline iron phosphide nanorods/ nanowires. *J. Am. Chem. Soc.*, 126, 1195–1198.

31. Hofmeister, H. (2004). Five-fold twinned nanoparticles. *Encyclopaedia of Nanosci. Nanotech.*, 3, 431–452.
32. Yacaman, M.J., Almazo, M.M. & Ascencio, J.A. (2001). High resolution TEM studies on palladium nanoparticles. *J. Mol. Catal. A: Chem.*, 173, 61–74.